DNA-based immobilization for improved electrochemical carbon dioxide reduction

Gang Fan,[1] Nathan Corbin,[1] Thomas M. Gill,[1] Amruta A. Karbelkar,[1] and Ariel L. Furst [1,2*]

1. Department of Chemical Engineering, Massachusetts Institute of Technology, Cambridge, MA 02139.

2. Center for Environmental Health Sciences, Massachusetts Institute of Technology, Cambridge, MA 02139.

ABSTRACT: Electrochemical reduction of carbon dioxide (CO_2) is a promising route for the up-conversion of this industrial by-product. However, to perform this reaction with a small-molecule catalyst, the catalyst must be proximal to an electrode surface. Efforts to immobilize these catalysts on electrodes have been stymied by the need to optimize immobilization chemistries on a case-by-case basis. As with many reactions, Nature has evolved catalysts with high specificity, selectivity, and activity. By taking inspiration from biological porphyrins and combining it with the specificity of DNA hybridization, we have developed an improved electrocatalyst platform for CO_2 reduction. The addition of single-stranded DNA to the porphyrin-based catalysts improved their stability, and DNA-catalyst conjugates were immobilized on screen-printed carbon electrodes using DNA hybridization with nearly 100% efficiency. Increased turnover frequency (TOF) and catalyst stability were observed with the DNA-immobilized catalysts as compared to the unmodified small molecules. This work demonstrates the importance of taking inspiration from Nature and demonstrates the potential of DNA hybridization as a general strategy for molecular catalyst immobilization.

An expected 500 gigatons of carbon dioxide (CO_2) will be produced in the next five decades as a major by-product of many industrial processes.[1] Despite its abundance and potential as a one-carbon feedstock, CO_2 has yet to be extensively applied to generate value-added chemicals.[2,3] The first step in this process is the reduction of CO_2 to generate carbon monoxide (CO), a key component of syngas (synthetic gas), which is used as a fuel source and as an intermediate for chemical production. Thus, significant effort has been devoted to the development of technologies to convert CO_2 to CO.[4–6] Electrochemical CO_2 reduction (ECR) is one of the most common methods of CO_2 conversion, with many examples of both homogeneous and heterogeneous systems.[1,7,8] Small molecule catalysts for ECR are advantageous because of their tunability and well-defined active sites.[9–11] These catalysts can be employed homogeneously, but their immobilization on electrodes is advantageous,[12,13] as it eliminates mass transport limitations due to catalyst diffusion and can improve the catalyst-electrode interactions.[8] In heterogeneous systems, both the local environment surrounding the catalyst and the ability of the substrate to reach it significantly impact the conversion efficiency and reaction products.[14,15,16]

Though synthetic catalysts are important, Nature has evolved enzymes that outperform these small molecules in many cases because of their inherent substrate specificity and reaction intermediate stabilization.[17,18] Thus, there has been significant effort to develop bio-inspired and bio-derived systems to improve synthetic catalysts.[19,20] One key structure found in many enzyme active sites is porphyrin, a core ligand structure that often chelates cobalt or iron in Nature.[21] This structure is found in enzymes ranging from oxygenases to peroxidases and is the catalytic core of engineered cytochromes capable of complex transformations.[21] Thus, we used this biological molecule as a starting point to improve CO_2 reduction. Using core porphyrin structures, molecular catalysts have been shown to be effective for CO_2RR, although their efficiency remains relatively low compared to other catalysts.

One strategy to improve catalysis is to immobilize small-molecule catalysts on electrode surfaces, generally either through direct grafting of a ligand to the electrode[14,22–26] or through non-covalent interaction between pyrene moieties and low-dimensional carbon surfaces.[27–29] However, these systems can be limited by substrate transport, and current densities are often lower than their homogeneous equivalents.[30] Just as we took inspiration from Nature for the catalysts selected, we sought to improve catalysis with these molecules using the inherent properties of DNA; because of its stability, chemical tunability, and inherent self-recognition, we used DNA as a "molecular Velcro" to immobilize molecular catalysts.

DNA is often thought of solely in the context of the genetic code, but its three-dimensional structure imbues it with unique materials properties beyond the central dogma of biology.[31–38] DNA is a naturally-occurring polymer comprised of two complementary oligonucleotide strands. These strands self-recognize as sequence-specific "Velcro." Further, once the DNA duplex is formed, the pi orbitals of the aromatic bases overlap to stabilize the structure of DNA b. This overlap further allows the DNA to conduct electrons as a molecular wire.[39–41] These properties have brought new opportunities in materials science,[34,42] sensing, and diagnostics.[43–45] Among them, DNA "Velcro" has been used to pattern cells[39,46–50] and antibodies.[32,51] Despite these advantages, DNA has yet been applied to energy-relevant catalysis.

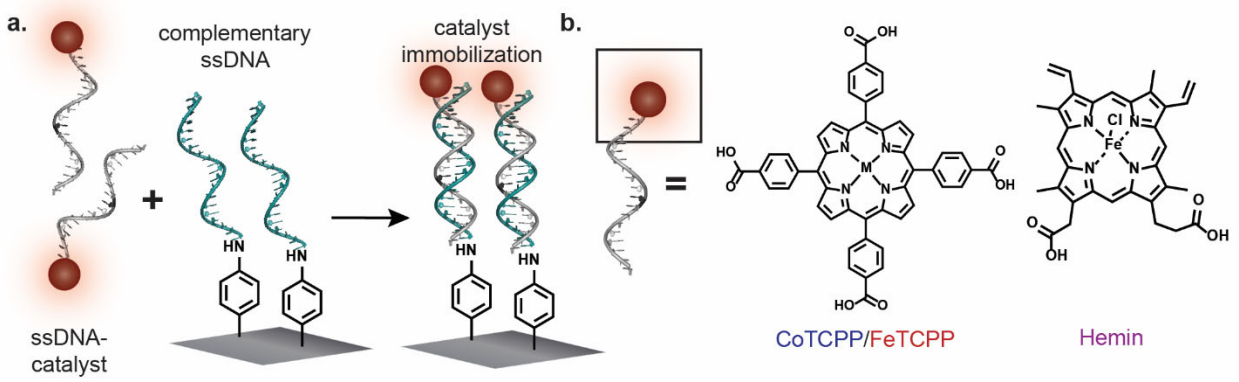

Figure 1. Catalyst immobilization using DNA "Velcro." a) Single-stranded DNA (ssDNA) conjugated to a small-molecule catalyst is hybridized to complementary DNA attached to a carbon electrode. b) The small-molecule catalysts evaluated include CoTCPP, FeTCPP, and hemin.

Here, we demonstrate the first application of DNA "Velcro" to immobilize molecular ECR catalysts on electrode surfaces (Figure 1). This immobilization strategy yields improved catalytic efficiency. The DNA-catalyst conjugates are readily synthesized and are found to have improved stability simply through single-stranded DNA addition. Subsequent immobilization on carbon electrodes through hybridization to pre-deposited complementary strands showed improved catalysis. We anticipate this method being a general strategy to improve aqueous catalysis.

Results and Discussion

ECR in solution with porphyrin-based catalysts

We selected three porphyrin-based catalysts (Co(II) and Fe(III) tetrakis(4-carboxyphenyl)porphyrin (H_2TCPP)--CoTCPP, and FeTCPP, and hemin, Figure 1b) due to their known catalytic properties, readily-understood mechanism of proton-coupled electron transfer (PCET), and ability to vary the metal incorporated into porphyrin derivatives.[52] Commercial hemin with the iron incorporated was used, and CoTCPP and FeTCPP were metalated with the corresponding metal ions from commercial H_2TCPP. Metalation was confirmed by mass spectrometry (Figure S4).

We initially investigated the CO_2 reduction reaction (CO_2RR) catalytic activity of these three porphyrin-derived catalysts in solution using screen-printed carbon electrodes (SPEs) in aqueous media. We selected carbonate electrolytes because of their prevalence as electrolytes for CO_2RR.[53–55] Additionally, the free porphyrin-based catalysts are soluble in these solvents at the concentrations used for the studies describes here. As seen in Figure 2, catalytic current is observed by cyclic voltammetry (CV) using 0.5 mM CoTCPP in aqueous buffer saturated with CO_2 at neutral pH. In the absence of CO_2, the observed current was three-fold lower than in its presence (Figure 2a). Similarly, the current generated by FeTCPP under the same conditions exhibited a two-fold increase when the buffer was saturated with CO_2. Under an N_2 atmosphere, three redox processes are observed. Peak A is attributed to the $Fe^{III/II}$ couple, while peaks B and C are attributed to the irreversible $Fe^{II/I}$ reduction and hydrogen evolution, respectively (Figure 2b). The increase in current observed in the $Fe^{I/0}$ potential region (-1.4- -1.3V vs AgCl/Ag) when CO_2 is present in the solution is indicative of CO_2RR.

In contrast to the TCPP-based catalysts, no significant difference in current was observed for 0.5 mM hemin in a 95% buffer/5% ACN solution either in the presence or absence of CO_2 (Figure 2c). This observation is explained by the inevitable competition between CO_2 reduction and hydrogen evolution in aqueous buffers. Indeed, the results from the chromatography analysis of the gaseous products generated in the headspace of the electrochemical cell indicated the CO production rates are relatively low with this catalyst (Figure S11). The turnover frequency (TOF) toward CO for these porphyrin-based catalysts were estimated to be 853 s^{-1} (CoTCPP), 16 s^{-1} (FeTCPP), and 164 s^{-1} (hemin) using standard foot-of-the-wave analysis and the measured faradaic efficiency at 1.4 V vs. AgCl/Ag (Figure 5, S14-16, detailed methods are described in SI).[56,57] Thus, these bio-inspired small-molecule catalysts are capable of ECR, but their efficiency is too low for broad utility. Further, the concentrations required for catalysis (often mM) are inefficient, making them unsuitable for larger-scale systems.

Importantly, though CO_2RR was observed for the TCPP-based catalysts, the highly variable currents observed by chronoamperometry for both CoTCPP and FeTCPP at -1.4 V vs AgCl/Ag (the potential at which CO_2RR occurs) indicate that catalyst decomposition and, potentially, precipitation onto the electrode occurs in this electrochemical potential regime (Figure 3). In contrast, the current observed by chronoamperometry for hemin remains stable at -1.4 V vs AgCl/Ag. This observed stability difference is to be expected based on the role of the porphyrin catalytic center in native biological systems. This finding compared to the relative instability of the synthetic porphyrin derivatives (TCPP-based catalysts) confirms the importance of looking to native biological systems for inspiration and guidance in catalyst design. Taken together, these data indicate that the homogeneous molecular catalysts in solution are unstable at the requisite potential for CO_2RR, making them unsuitable for ECR at scale.

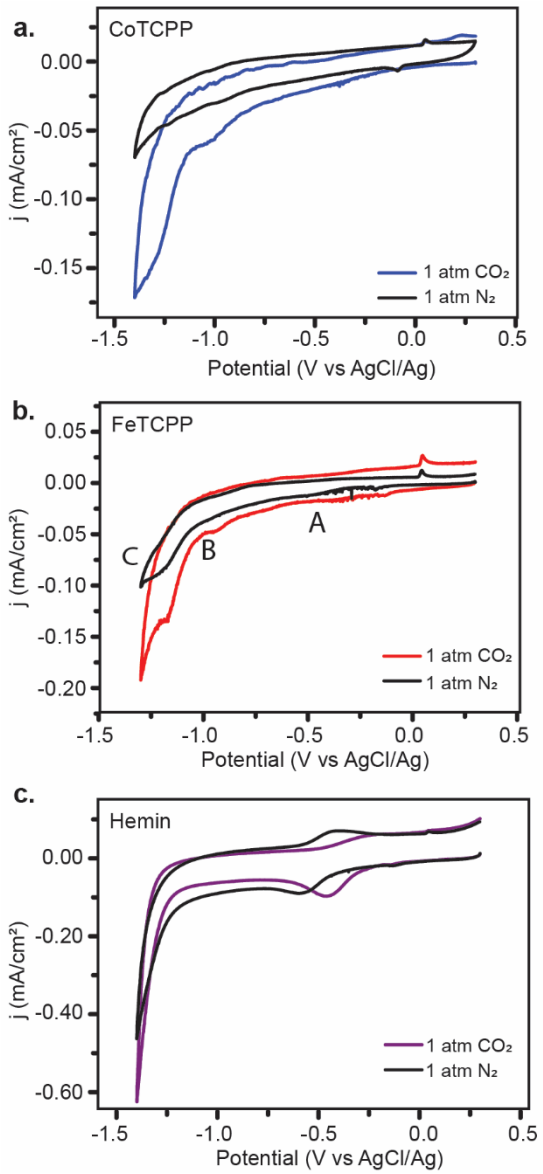

Figure 2. Homogeneous electrochemical CO_2 reduction in aqueous buffers. a-c) Cyclic voltammetry (CV) of CoTCPP, FeTCPP or Hemin (0.5 mM total concentration), under nitrogen (black) and CO_2 (colored), carried out at a scan rate of 100 mVs^{-1}, on screen-printed electrodes. The electrolyte is KCl (0.1 M) and K_2CO_3 (0.5 M) at pH 7.4, adjusted by adding aliquots of HCl.

Synthesis and optimization of DNA-catalyst conjugates

Based on the observed limitations with the small-molecule catalysts, improving their stability and increasing their efficiency were identified as key needs. Although we took inspiration from enzyme active sites for the selection of catalysts, enzymes are often highly susceptible to inactivation from temperature fluctuations, pH changes, and the relative ionic strength of the solution in which they are maintained. Further, proteins can be challenging to generate at scale without significant process optimization and costly purification. Thus, to improve the stability and system control, we turned to another important biomolecule: DNA. As DNA is highly stable under diverse aqueous conditions (a wide range of temperatures, pH's, and ionic strengths), tunable, and synthetically tractable, it was an optimal choice as an addition to molecular catalysts that suffer from aqueous solubility issues and limited stability.

To investigate the impact of DNA on ECR with the porphyrin-based catalysts, we synthesized catalyst-oligonucleotide conjugates, which we term single-stranded DNA (ssDNA) conjugates. Traditional bioconjugation strategies were undertaken involving amide bond formation between the catalyst ligand containing carboxylic acids and amine-terminated ssDNA (Figure S1). Porphyrin-DNA conjugates were initially reported nearly three decades ago by Meunier *et al.*[58] and Heĺeǹe *et al.*[59] but have mainly been used in fundamental scientific studies (*e.g.*, for DNA sensing[60] and inter-strand crosslinking[61]). The relatively narrow range of applications to-date is attributed to challenging synthesis, intermolecular interactions that can lead to aggregation, and solubility issues. Indeed, we initially chose the prevalent amide coupling conditions[62] (1-ethyl-3-(3-(dimethylamino)propyl)carbodiimide (EDC), 1-hydroxybenzotriazole (HOBt) and DIPEA) and found no noticeable conversion with any of the three molecular catalysts. We therefore evaluated a variety of prevalent reagents for amide bond formation and found that the majority of the established reagents resulted in very low yields for this reaction. The highest yields were consistently found with a combination of hexafluorophosphate azabenzotriazole tetramethyl uronium and N,N'-diisopropylethylamine (HATU/DIPEA) reagents, which provide decent conversion for all three ssDNA-catalyst conjugates. The matrix-assisted laser desorption/ionization time-of-flight (MALDI-TOF) mass spectrometry and reverse phase high performance liquid chromatography (RP-HPLC) confirmed the successful synthesis and purification of the hemin- and Co/FeTCPP-DNA conjugates (Figure S5-S6). Despite the prevalence of this reaction for bioconjugations and the similarity of the core ligand structures for the three catalysts evaluated, we observed significant differences in the efficacy of standard reagents based on the catalyst being conjugated. This observation is worth noting for the expansion of this technology to additional catalysts, as some optimization may be required for the coupling.

DNA-modified catalyst electrochemistry in solution

The challenges in optimizing coupling conditions highlighted one of the key drawbacks of porphyrin derivatives: their limited solubility in aqueous buffers. However, following DNA modification, we observed an interesting phenomenon: a significant increase in the aqueous solubility of the catalysts. Thus, though our ultimate goal was to immobilize these catalysts on electrodes using DNA "Velcro," we first sought to investigate the impact of DNA addition to the catalysts in solution. We evaluated the stability of the conjugates, as well as their ability to perform CO_2RR, in solution. When compared to the largely insoluble small-molecule catalysts, the DNA conjugates were found to be highly soluble in aqueous buffers without the addition of co-solvents. This is a significant finding, as fully aqueous-soluble catalysts allow for additional flexibility in the pH and buffering conditions that can be used with the system. Both of these variables significantly impact CO_2RR efficiency independent of

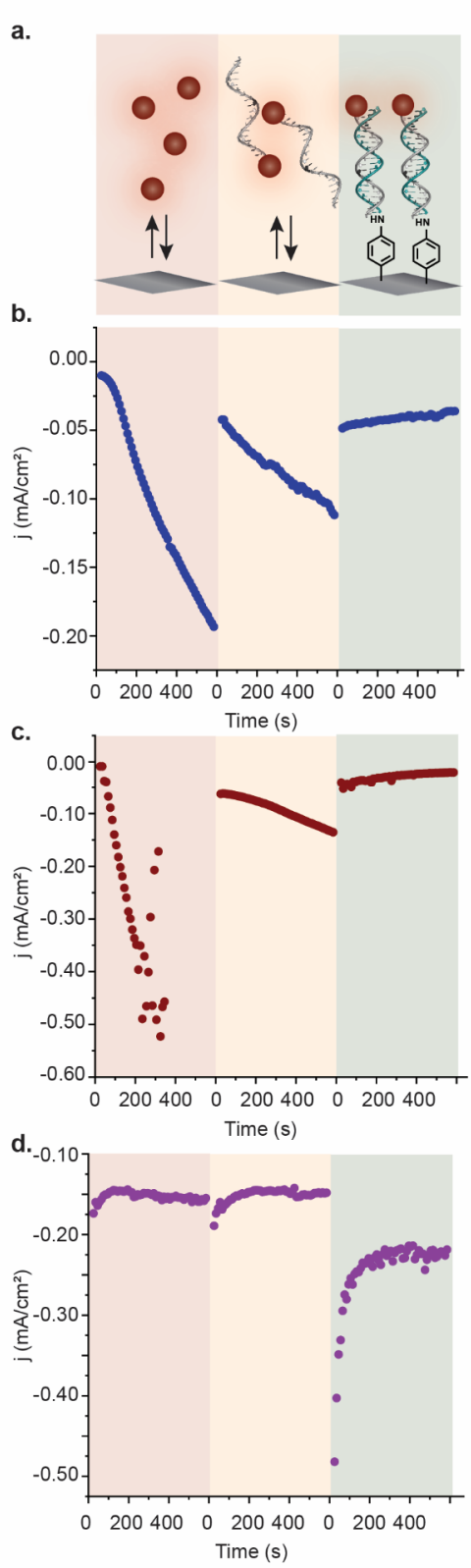

Figure 3. Stability comparison between free catalyst, ssDNA-modified catalyst, and dsDNA immobilized catalyst. a) Schematic of catalysts. b-d) Chronoamperometry of catalysts in the three conditions at -1.4 V vs. AgCl/Ag. Experiments were performed on carbon SPEs, and the electrolyte used was KCl (0.1 M) and K_2CO_3 (0.5 M) at pH 7.4, adjusted by adding aliquots of HCl.

the catalyst, making the ability to tune these parameters without solubility concerns a significant advantage of this method.[63] Given our results, we anticipate that a range of energy-relevant conversions could be improved through catalyst modification with DNA.

What was somewhat surprising and an important result was the immediate and significant improvement in the stability of the TCPP-derived catalysts simply through the addition of DNA. The hemin catalyst demonstrated similar stability to the unmodified version, which is unsurprising, as the catalyst was stable in the absence of the ssDNA; it is worth noting, though, that the presence of the DNA did not destabilize this catalyst. Under the same electrochemical conditions as were used to evaluate the unmodified porphyrin catalysts, the DNA-modified catalysts maintained their activity and remained stable at potentials that caused degradation for the small-molecule catalysts alone (Figure 3, S8). Thus, simply adding the soluble oligonucleotide significantly improved the stability of the catalysts in solution (Figure 3). Although solvent effects are established in ECR catalysis, this finding supports the importance of the local environment beyond simply the pH and ionic strength surrounding the metal center on the stability of the small molecules.

Upon monitoring catalysis with these conjugate, we observed that the turnover for the ssDNA conjugates was lower than that of the free catalyst in solution. The TOFs of CoTCPP-DNA, FeTCPP-DNA, and hemin-DNA for homogenous, ssDNA-electrocatalysis were calculated to be 24.7 s^{-1}, 6.2 s^{-1} and 20.9 s^{-1} respectively, which is lower than those found for the free catalysts (Figure 5, S14-16). We attribute this to the increased size of the DNA-catalyst conjugate compared to the small molecule alone, decreasing the relative rate of diffusion. Despite decreased TOF, the incorporation of ssDNA to catalysts in solution did solve one of the two key challenges with these porphyrin-derived catalysts: stability. The next step was therefore to tackle the overall efficiency of catalysis, which we anticipated would be improved through the application of DNA "Velcro" to immobilize the catalysts on electrodes.

Surface modification with DNA

Prior to surface immobilization of the ssDNA-catalyst conjugates, electrodes stably modified with complementary DNA were needed. Conventionally, biomolecule modification on electrodes is performed on gold electrodes due to their ease of modification with any biomolecule containing a free thiol. Despite this ease, gold surfaces of sufficient quality for modification are costly, the accessible potential window is smaller than that of other materials such as carbon, and the gold-thiol bond formed is relatively unstable and susceptible to reductive stripping. Thus, for the potentials required for CO_2RR, gold was an unsuitable material. We therefore developed and recently reported new chemistry to modify carbon electrodes with biomolecules using an oxidative coupling bioconjugation reaction.[64]

We applied this workflow to modify disposable SPEs with ssDNA (complementary to DNA-catalyst conjugates) by oxidative coupling between *o*-aminophenol-modified DNA

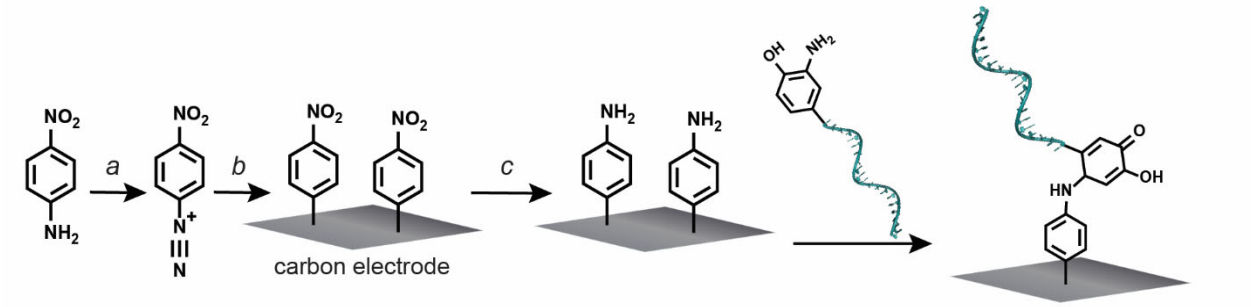

Scheme 1. A *p*-nitroaniline is used as a chemical handle for DNA attachment. To modify an electrode with anilines, an *in situ* diazonium is generated (*a*). Upon electrochemical reduction, a carbon-carbon bond is generated between the nitrobenzyl moiety and an electrode surface (*b*). Electrochemical reduction is again used to reduce the nitrobenzyl group to an aniline on the surface (*c*). Aminophenol-DNA is then directly tethered to the modified electrode.

and aniline-modified surfaces. This reaction proceeds in the presence of a mild oxidant: potassium ferricyanide (Scheme 1).[65] To perform this reaction, commercial synthetic DNA containing a terminal amine was first modified with an *o*-nitrophenol appended with a carboxylic acid. The *o*-nitrophenol was then reduced to an *o*-aminophenol, which was synthesized as previously described.[64] Following size exclusion purification, a single peak observed by MALDI-TOF measurement indicated near-quantitative conversion to *o*-aminophenol-ssDNA (Figure S7).

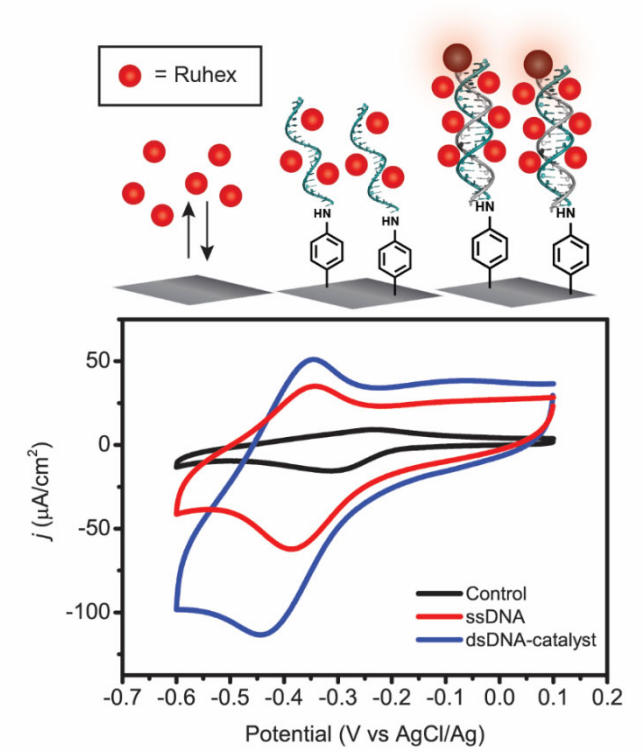

Figure 4. a) Oxidative coupling reaction of aniline with o-aminophenol ssDNA conjugates and then hybridized with complementary ssDNA-catalyst. The ruthenium ions interact electrostatically with the DNA backbone to act as a phosphate counter. b) CV of catalyst-ssDNA-functionalized (blue), ssDNA modified (red) or uncoated (black) SPE in a stock solution (10 mM Tris buffer, pH 7.4, containing 2 μM RuHex), carried out at a scan rate of 500 mV·s^{-1}.

Preparation of aniline-modified electrodes as the coupling partner was achieved by electrochemically-induced grafting of *o*-nitroaniline through the generation of a diazonium salt and subsequent reduction of the resultant nitrobenzyl at the surface to an aniline moiety. The successful electrode modification was confirmed by characteristic reductive peaks observed in the CV (-0.05V vs AgCl/Ag, and -0.9 V vs AgCl/Ag respectively; Figure S2). Subsequent coupling of ssDNA to aniline-modified SPEs using ferricyanide was confirmed by hexaammineruthenium (RuHex) DNA quantification. RuHex interacts electrostatically with the DNA backbone to act as a phosphate counter (Figure 4, S3). From these results, the surface concentration of oligonucleotides was calculated to be (7.2 ± 3.0) × 10^{-12} mol/cm^2 (Figure S3, detailed methods are described in SI).[66] This is well within the standard DNA coverages observed using conventional gold-thiol chemistries, which generally range from 1-100 pmol/cm^2.[40,41,67] Thus, the maximum surface density of catalyst loading on the electrode following hybridization is 7.2 pmol/cm^2. Confirmation of consistent carbon electrode modification with DNA, especially because low-cost screen-printed electrodes were used in this study, is essential to the success of immobilization of reductive electrocatalysts on electrodes.

Hybridization to surface and differences in catalysis

Having successfully modified SPEs with ssDNA, we next examined CO_2RR efficiency upon catalyst immobilization on electrodes through DNA hybridization, or DNA "Velcro." Both DNA-modified electrodes and complementary DNA-catalyst conjugates were heated to 65 °C, and the ssDNA-catalyst conjugate was added to the complementary DNA-modified electrode. The electrode was then slowly cooled to room temperature over one hour, and the unbound catalyst-DNA conjugates were removed by repeated washing. We then use cyclic voltammetry to monitor the surface hybridization by RuHex DNA quantification. Impressively, the total charge obtained by integration of the redox peaks in the cyclic voltammograms was calculated to be 1.64 μC after catalyst-DNA hybridization, whereas the total charge from the ssDNA-modified SPE was determined to be 0.84 μC (Figure 4). Thus, the surface density of catalyst is estimated to be 6.4 pmol/cm^2, achieving a near-unity hybridization efficiency (the surface concentration of single-strand oligonucleotides on SPE surface was calculated to be 6.5

pmol/cm^2). Moreover, in presence of CO_2, a ten-fold increase in current was observed by chronoamperometry for the catalyst-modified electrode in KCl/K_2CO_3 buffer as compared to the electrode modified only with ssDNA. These data indicate that the catalyst-DNA was successfully immobilized on the electrode through DNA hybridization and that the hybridization maintained the activity of the catalyst (Figure S10). This observation is important, as altering the activity or accessibility of biomolecules following immobilization on surfaces is always a concern, and establishing that they maintain their desired activity is important.

As compared to the homogeneous catalysts in solution, the DNA-immobilized catalysts demonstrated both improved stability and CO_2RR efficiency. Surprisingly, for DNA-immobilized CoTCPP, steady currents were observed by chronoamperometry at significantly negative potentials (-1.5 V vs AgCl/Ag), indicating that DNA "Velcro" leads to improved CO_2RR catalyst stability (Figure S9). Both FeTCPP and hemin immobilized with DNA showed stable currents at relevant potentials for CO_2RR (-1.4 V vs AgCl/Ag), while homogenous catalysts showed degradation at this potential (Figure 3). For FeTCPP immobilized with DNA, CO_2 electrocatalysis was observed at a less negative overpotential (-1.15 V vs AgCl/Ag), and quasi-quantitative CO formation was observed by GC with minimal hydrogen evolution (Figure S13). This observation of CO by gas chromatography (GC) further confirms that the catalysts remain active on electrode, as no CO production was observed for DNA-modified electrodes alone (Figure S12). Impressively, the amount of CO generated from the picomoles/cm^2 of catalyst immobilized on the electrode is comparable to the amount generated from micromolar concentrations of homogenous catalyst in solution (Figure S11). The TOF of hemin immobilized with DNA demonstrated a nearly 10^3-fold increase (1.01×10^5 s^{-1}) compared to the homogenous molecular catalysts (Figure 5, S14-16). Similarly, the TOF of the FeTCPP and CoTCPP immobilized with DNA demonstrated 100- and 10- fold increases (7.42×10^3 s^{-1} and 7.48×10^3 s^{-1}), respectively (Figure 5, S14-16). The immobilization of ssDNA-catalyst conjugates on electrodes had the intended effect: TOF while maintaining the improved stability observed with ssDNA-catalyst conjugates in solution. Taken together, these results demonstrate the circumvention of key challenges in CO_2RR with small-molecule catalysts: stability and efficiency.

The elegance of enzymatic reactions has inspired the incorporation of biomolecules such as amino acids and peptides with CO_2RR catalysis to improve selectivity and solubility.[20,68,69] In this study, we took inspiration from Nature and evaluated the ability of DNA to serve as a molecular "Velcro" to tether bio-inspired small-molecule ECR catalysts to electrodes. For the metalloporphyrin catalysts employed in this study, the efficiency of ECR for the desired CO product is closely related to the microenvironment surrounding the metal centers. We theorize that the improved ECR efficiency observed in our system is due to alterations in the outer coordination sphere resulting from the presence of DNA. Moreover, we observed that, for DNA-immobilized FeTCPP, ECR could be carried out at a less negative potential than for the homogeneous catalysis (-1.15 V vs AgCl/Ag), which is likely due to the increased stability and solvent accessibility of the catalyst.

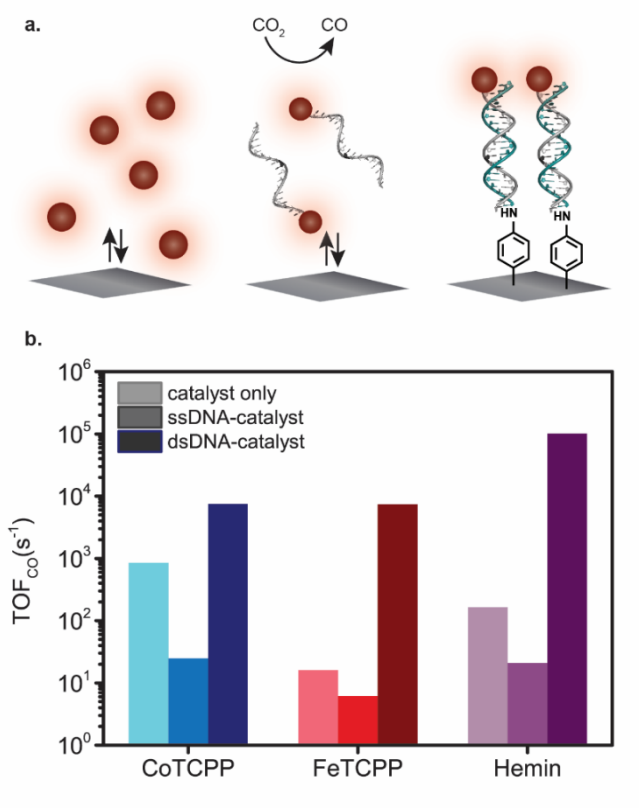

Figure 5. DNA-modified electrochemistry in solution and on an electrode. a) Schematic representation of free catalyst, DNA-modified catalyst in solution or hybridized onto the electrode surface. b) On-line gas chromatography (GC) analysis. TOF of CO generated by free catalyst, DNA-modified catalyst in solution and on electrode (CO_2 flow rate: 10 sccm), carried out at -1.5 V vs. AgCl/Ag on carbon SPEs. The electrolyte is KCl (0.1 M) and K_2CO_3 (0.5 M) at pH 7.4, adjusted by adding aliquots of HCl.

Overall, we have demonstrated that DNA "Velcro" to tether catalysts to electrodes improves their efficiency and stability. The readily-synthesized catalyst-ssDNA conjugates afford improved aqueous solubility and enhanced stability. Furthermore, the DNA hybridization-based CO_2RR catalyst immobilization yielded systems with higher TOF compared to the unmodified controls. Taken together, our results provide an important proof-of-principle demonstration of the power of DNA "Velcro" to improve catalysis. We anticipate that this platform will be a powerful tool to enable increased activity and stability of many additional important classes of catalysts.

Materials and Methods:

Functionalization of amino-modified DNAs with metalated TCPP catalyst by HATU/DIPEA method: In a typical reaction, to a solution of amino-modified DNA (2.0 nmol) in MOPS buffer (300 µL, 50 mM, 0.5 M NaCl, pH 8.0) was added a mixture of FeTCPP (0.2 mg, 240 nmol), HATU (0.8 mg, 2.1 µmol), and DIPEA (0.4 µL, 2.1 µmol) in 300 µL DMF at room temperature. The reaction was agitated for 24 hours and resulted in covalent attachment of the FeTCPP complex to the DNA. The DNA-catalyst

conjugates were then purified by reverse-phase HPLC using a water (50mM TEAA) (solvent A)/ACN (solvent B) gradient and characterized by MALDI-TOF mass spectrometry.

Safety considerations: No unexpected or unusually high safety hazards were encountered.

ASSOCIATED CONTENT

Methods and materials, supplemental figures, and supplemental references are available.

AUTHOR INFORMATION

Corresponding Author

*Ariel Furst; afurst@mit.edu

Author Contributions

The manuscript was written through contributions of all authors.

Funding Sources

We acknowledge the MIT Energy Initiative for funding this work. N.C. was funded by a grant from the National Science Foundation (no. 1955628).

ACKNOWLEDGMENTS

We acknowledge the MIT Energy Initiative for funding this work. N.C. was funded by a grant from the National Science Foundation (no. 1955628).

REFERENCES

(1) Aresta, M.; Dibenedetto, A. Utilisation of CO2 as a Chemical Feedstock: Opportunities and Challenges. *Dalt. Trans.* **2007**, No. 28, 2975–2992. https://doi.org/10.1039/B700658F.

(2) Koytsoumpa, E. I.; Bergins, C.; Kakaras, E. The CO2 Economy: Review of CO2 Capture and Reuse Technologies. *J. Supercrit. Fluids* **2018**, *132*, 3–16. https://doi.org/https://doi.org/10.1016/j.supflu.2017.07.029.

(3) Salimijazi, F.; Kim, J.; Schmitz, A. M.; Grenville, R.; Bocarsly, A.; Barstow, B. Constraints on the Efficiency of Engineered Electromicrobial Production. *Joule* **2020**. https://doi.org/10.1016/j.joule.2020.08.010.

(4) Heidlage, M. G.; Kezar, E. A.; Snow, K. C.; Pfromm, P. H. Thermochemical Synthesis of Ammonia and Syngas from Natural Gas at Atmospheric Pressure. *Ind. Eng. Chem. Res.* **2017**, *56* (47), 14014–14024. https://doi.org/10.1021/acs.iecr.7b03173.

(5) Dry, M. E. The Fischer–Tropsch Process: 1950–2000. *Catal. Today* **2002**, *71* (3), 227–241. https://doi.org/https://doi.org/10.1016/S0920-5861(01)00453-9.

(6) Dry, M. E. Practical and Theoretical Aspects of the Catalytic Fischer-Tropsch Process. *Appl. Catal. A Gen.* **1996**, *138* (2), 319–344. https://doi.org/https://doi.org/10.1016/0926-860X(95)00306-1.

(7) Abdulaeva, I. A.; Birin, K. P.; Michalak, J.; Romieu, A.; Stern, C.; Bessmertnykh-Lemeune, A.; Guilard, R.; Gorbunova, Y. G.; Tsivadze, A. Y. On the Synthesis of Functionalized Porphyrins and Porphyrin Conjugates via β-Aminoporphyrins. *New J. Chem.* **2016**, *40* (7), 5758–5774. https://doi.org/10.1039/C5NJ03247D.

(8) Corbin, N.; Zeng, J.; Williams, K.; Manthiram, K. Heterogeneous Molecular Catalysts for Electrocatalytic CO2 Reduction. *Nano Res.* **2019**, *12* (9), 2093–2125. https://doi.org/10.1007/s12274-019-2403-y.

(9) Benson, E. E.; Kubiak, C. P.; Sathrum, A. J.; Smieja, J. M. Electrocatalytic and Homogeneous Approaches to Conversion of CO2 to Liquid Fuels. *Chem. Soc. Rev.* **2009**, *38* (1), 89–99. https://doi.org/10.1039/b804323j.

(10) Nielsen, D. U.; Hu, X.-M.; Daasbjerg, K.; Skrydstrup, T. Chemically and Electrochemically Catalysed Conversion of CO2 to CO with Follow-up Utilization to Value-Added Chemicals. *Nat. Catal.* **2018**, *1* (4), 244–254. https://doi.org/10.1038/s41929-018-0051-3.

(11) Hori, Y.; Murata, A.; Kikuchi, K.; Suzuki, S. Electrochemical Reduction of Carbon Dioxides to Carbon Monoxide at a Gold Electrode in Aqueous Potassium Hydrogen Carbonate. *J. Chem. Soc. Chem. Commun.* **1987**, No. 10, 728–729. https://doi.org/10.1039/C39870000728.

(12) Liu, Y.; Leung, K. Y.; Michaud, S. E.; Soucy, T. L.; McCrory, C. C. L. Controlled Substrate Transport to Electrocatalyst Active Sites for Enhanced Selectivity in the Carbon Dioxide Reduction Reaction. *Comments Inorg. Chem.* **2019**, *39* (5), 242–269. https://doi.org/10.1080/02603594.2019.1628025.

(13) Kramer, W. W.; McCrory, C. C. L. Polymer Coordination Promotes Selective CO2 Reduction by Cobalt Phthalocyanine. *Chem. Sci.* **2016**, *7* (4), 2506–2515. https://doi.org/10.1039/C5SC04015A.

(14) Oh, S.; Gallagher, J. R.; Miller, J. T.; Surendranath, Y. Graphite-Conjugated Rhenium Catalysts for Carbon Dioxide Reduction. *J. Am. Chem. Soc.* **2016**, *138* (6), 1820–1823. https://doi.org/10.1021/jacs.5b13080.

(15) Hu, X.-M.; Rønne, M. H.; Pedersen, S. U.; Skrydstrup, T.; Daasbjerg, K. Enhanced Catalytic Activity of Cobalt Porphyrin in CO2 Electroreduction upon Immobilization on Carbon Materials. *Angew. Chemie Int. Ed.* **2017**, *56* (23), 6468–6472. https://doi.org/10.1002/anie.201701104.

(16) Austin, N.; Zhao, S.; McKone, J. R.; Jin, R.; Mpourmpakis, G. Elucidating the Active Sites for CO2 Electroreduction on Ligand-Protected Au25 Nanoclusters. *Catal. Sci. Technol.* **2018**, *8* (15), 3795–3805. https://doi.org/10.1039/C8CY01099D.

(17) Chen, K.; Arnold, F. H. Engineering New Catalytic Activities in Enzymes. *Nat. Catal.* **2020**, *3* (3), 203–213. https://doi.org/10.1038/s41929-019-0385-5.

(18) Chen, J. G.; Crooks, R. M.; Seefeldt, L. C.; Bren, K. L.; Bullock, R. M.; Darensbourg, M. Y.; Holland, P. L.; Hoffman, B.; Janik, M. J.; Jones, A. K.; et al. Beyond Fossil Fuel–Driven Nitrogen Transformations. *Science (80-.).* **2018**, *360* (6391), eaar6611. https://doi.org/10.1126/science.aar6611.

(19) Le, J. M.; Bren, K. L. Engineered Enzymes and Bioinspired Catalysts for Energy Conversion. *ACS Energy Lett.* **2019**, *4* (9), 2168–2180. https://doi.org/10.1021/acsenergylett.9b01308.

(20) Fan, G.; Wasuwanich, P.; Furst, A. L. Biohybrid Systems for Improved Bioinspired, Energy-Relevant Catalysis. *ChemBioChem* **2021**, *n/a* (n/a). https://doi.org/https://doi.org/10.1002/cbic.202100037.

(21) Prier, C. K.; Arnold, F. H. Chemomimetic Biocatalysis: Exploiting the Synthetic Potential of Cofactor-Dependent Enzymes To Create New Catalysts. *J. Am. Chem. Soc.* **2015**, *137* (44), 13992–14006. https://doi.org/10.1021/jacs.5b09348.

(22) Elgrishi, N.; Griveau, S.; Chambers, M. B.; Bedioui, F.; Fontecave, M. Versatile Functionalization of Carbon Electrodes with a Polypyridine Ligand: Metallation and Electrocatalytic H+ and CO2 Reduction. *Chem. Commun.* **2015**, *51* (14), 2995–2998. https://doi.org/10.1039/C4CC10027A.

(23) Atoguchi, T.; Aramata, A.; Kazusaka, A.; Enyo, M. Electrocatalytic Activity of CoII TPP-Pyridine Complex Modified Carbon Electrode for CO2 Reduction. *J. Electroanal.*

Chem. Interfacial Electrochem. **1991**, *318* (1), 309–320. https://doi.org/https://doi.org/10.1016/0022-0728(91)85312-D.

(24) Atoguchi, T.; Aramata, A.; Kazusaka, A.; Enyo, M. Cobalt(II)–Tetraphenylporphyrin–Pyridine Complex Fixed on a Glassy Carbon Electrode and Its Prominent Catalytic Activity for Reduction of Carbon Dioxide. *J. Chem. Soc. Chem. Commun.* **1991**, No. 3, 156–157. https://doi.org/10.1039/C39910000156.

(25) Tanaka, H.; Aramata, A. Aminopyridyl Cation Radical Method for Bridging between Metal Complex and Glassy Carbon: Cobalt(II) Tetraphenylporphyrin Bonded on Glassy Carbon for Enhancement of CO2 Electroreduction. *J. Electroanal. Chem.* **1997**, *437* (1), 29–35. https://doi.org/https://doi.org/10.1016/S0022-0728(97)00080-6.

(26) Mohamed, E. A.; Zahran, Z. N.; Naruta, Y. Efficient Heterogeneous CO2 to CO Conversion with a Phosphonic Acid Fabricated Cofacial Iron Porphyrin Dimer. *Chem. Mater.* **2017**, *29* (17), 7140–7150. https://doi.org/10.1021/acs.chemmater.7b01115.

(27) Blakemore, J. D.; Gupta, A.; Warren, J. J.; Brunschwig, B. S.; Gray, H. B. Noncovalent Immobilization of Electrocatalysts on Carbon Electrodes for Fuel Production. *J. Am. Chem. Soc.* **2013**, *135* (49), 18288–18291. https://doi.org/10.1021/ja4099609.

(28) Kang, P.; Zhang, S.; Meyer, T. J.; Brookhart, M. Rapid Selective Electrocatalytic Reduction of Carbon Dioxide to Formate by an Iridium Pincer Catalyst Immobilized on Carbon Nanotube Electrodes. *Angew. Chemie Int. Ed.* **2014**, *53* (33), 8709–8713. https://doi.org/10.1002/anie.201310722.

(29) Maurin, A.; Robert, M. Noncovalent Immobilization of a Molecular Iron-Based Electrocatalyst on Carbon Electrodes for Selective, Efficient CO2-to-CO Conversion in Water. *J. Am. Chem. Soc.* **2016**, *138* (8), 2492–2495. https://doi.org/10.1021/jacs.5b12652.

(30) Kornienko, N.; Zhao, Y.; Kley, C. S.; Zhu, C.; Kim, D.; Lin, S.; Chang, C. J.; Yaghi, O. M.; Yang, P. Metal–Organic Frameworks for Electrocatalytic Reduction of Carbon Dioxide. *J. Am. Chem. Soc.* **2015**, *137* (44), 14129–14135. https://doi.org/10.1021/jacs.5b08212.

(31) Chidchob, P.; Edwardson, T. G. W.; Serpell, C. J.; Sleiman, H. F. Synergy of Two Assembly Languages in DNA Nanostructures: Self-Assembly of Sequence-Defined Polymers on DNA Cages. *J. Am. Chem. Soc.* **2016**, *138* (13), 4416–4425. https://doi.org/10.1021/jacs.5b12953.

(32) Jones, M. R.; Seeman, N. C.; Mirkin, C. A. Programmable Materials and the Nature of the DNA Bond. *Science (80-.).* **2015**, *347* (6224), 1260901. https://doi.org/10.1126/science.1260901.

(33) Hamblin, G. D.; Hariri, A. A.; Carneiro, K. M. M.; Lau, K. L.; Cosa, G.; Sleiman, H. F. Simple Design for DNA Nanotubes from a Minimal Set of Unmodified Strands: Rapid, Room-Temperature Assembly and Readily Tunable Structure. *ACS Nano* **2013**, *7* (4), 3022–3028. https://doi.org/10.1021/nn4006329.

(34) Macfarlane, R. J.; Jones, M. R.; Senesi, A. J.; Young, K. L.; Lee, B.; Wu, J.; Mirkin, C. A. Establishing the Design Rules for DNA-Mediated Programmable Colloidal Crystallization. *Angew. Chemie Int. Ed.* **2010**, *49* (27), 4589–4592. https://doi.org/10.1002/anie.201000633.

(35) Wang, P.; Meyer, T. A.; Pan, V.; Dutta, P. K.; Ke, Y. The Beauty and Utility of DNA Origami. *Chem* **2017**, *2* (3), 359–382. https://doi.org/https://doi.org/10.1016/j.chempr.2017.02.009.

(36) Aldaye, F. A.; Sleiman, H. F. Modular Access to Structurally Switchable 3D Discrete DNA Assemblies. *J. Am. Chem. Soc.* **2007**, *129* (44), 13376–13377. https://doi.org/10.1021/ja075966q.

(37) McLaughlin, C. K.; Hamblin, G. D.; Sleiman, H. F. Supramolecular DNA Assembly. *Chem. Soc. Rev.* **2011**, *40* (12), 5647–5656. https://doi.org/10.1039/C1CS15253J.

(38) Buchberger, A.; Simmons, C. R.; Fahmi, N. E.; Freeman, R.; Stephanopoulos, N. Hierarchical Assembly of Nucleic Acid/Coiled-Coil Peptide Nanostructures. *J. Am. Chem. Soc.* **2020**, *142* (3), 1406–1416. https://doi.org/10.1021/jacs.9b11158.

(39) Furst, A. L.; Smith, M. J.; Lee, M. C.; Francis, M. B. DNA Hybridization To Interface Current-Producing Cells with Electrode Surfaces. *ACS Cent. Sci.* **2018**, *4* (7), 880–884. https://doi.org/10.1021/acscentsci.8b00255.

(40) Furst, A.; Landefeld, S.; Hill, M. G.; Barton, J. K. Electrochemical Patterning and Detection of DNA Arrays on a Two-Electrode Platform. *J. Am. Chem. Soc.* **2013**, *135* (51), 19099–19102. https://doi.org/10.1021/ja410902j.

(41) Nano, A.; Furst, A. L.; Hill, M. G.; Barton, J. K. DNA Electrochemistry: Charge-Transport Pathways through DNA Films on Gold. *Cite This J. Am. Chem. Soc* **2021**, *143*. https://doi.org/10.1021/jacs.1c04713.

(42) Jones, M. R.; Seeman, N. C.; Mirkin, C. A. Programmable Materials and the Nature of the DNA Bond. *Science (80-.).* **2015**, *347* (6224), 1260901. https://doi.org/10.1126/science.1260901.

(43) Boal, A. K.; Barton, J. K. Electrochemical Detection of Lesions in DNA. *Bioconjug. Chem.* **2005**, *16* (2), 312–321. https://doi.org/10.1021/bc0497362.

(44) Furst, A. L.; Barton, J. K. DNA Electrochemistry Shows DNMT1 Methyltransferase Hyperactivity in Colorectal Tumors. *Chem. Biol.* **2015**, *22* (7), 938–945. https://doi.org/https://doi.org/10.1016/j.chembiol.2015.05.019.

(45) Furst, A. L.; Muren, N. B.; Hill, M. G.; Barton, J. K. Label-Free Electrochemical Detection of Human Methyltransferase from Tumors. *Proc. Natl. Acad. Sci. U. S. A.* **2014**, *111* (42), 14985–14989. https://doi.org/10.1073/pnas.1417351111.

(46) Douglas, E. S.; Chandra, R. A.; Bertozzi, C. R.; Mathies, R. A.; Francis, M. B. Self-Assembled Cellular Microarrays Patterned Using DNA Barcodes. *Lab Chip* **2007**, *7* (11), 1442–1448. https://doi.org/10.1039/b708666k.

(47) Furst, A. L.; Klass, S. H.; Francis, M. B. DNA Hybridization to Control Cellular Interactions. *Trends Biochem. Sci.* **2019**, *44* (4), 342–350. https://doi.org/10.1016/j.tibs.2018.10.002.

(48) Hsiao, S. C.; Shum, B. J.; Onoe, H.; Douglas, E. S.; Gartner, Z. J.; Mathies, R. A.; Bertozzi, C. R.; Francis, M. B. Direct Cell Surface Modification with DNA for the Capture of Primary Cells and the Investigation of Myotube Formation on Defined Patterns. *Langmuir* **2009**, *25* (12), 6985–6991. https://doi.org/10.1021/la900150n.

(49) Douglas, E. S.; Hsiao, S. C.; Onoe, H.; Bertozzi, C. R.; Francis, M. B.; Mathies, R. A. DNA-Barcode Directed Capture and Electrochemical Metabolic Analysis of Single Mammalian Cells on a Microelectrode Array. *Lab Chip* **2009**, *9* (14), 2010–2015. https://doi.org/10.1039/B821690H.

(50) Twite, A. A.; Hsiao, S. C.; Onoe, H.; Mathies, R. A.; Francis, M. B. Direct Attachment of Microbial Organisms to Material Surfaces through Sequence-Specific DNA Hybridization. *Adv. Mater.* **2012**, *24* (18), 2380–2385. https://doi.org/10.1002/adma.201104336.

(51) Palla, K. S.; Hurlburt, T. J.; Buyanin, A. M.; Somorjai, G. A.; Francis, M. B. Site-Selective Oxidative Coupling Reactions for the Attachment of Enzymes to Glass Surfaces through DNA-Directed Immobilization. *J. Am. Chem. Soc.* **2017**, *139* (5), 1967–1974. https://doi.org/10.1021/jacs.6b11716.

(52) Fukuzumi, S.; Lee, Y. M.; Ahn, H. S.; Nam, W. Mechanisms of Catalytic Reduction of CO2 with Heme and Nonheme Metal Complexes. *Chem. Sci.* **2018**, *9* (28), 6017–6034. https://doi.org/10.1039/c8sc02220h.

(53) Zhu, M.; Ye, R.; Jin, K.; Lazouski, N.; Manthiram, K. Elucidating

the Reactivity and Mechanism of CO2 Electroreduction at Highly Dispersed Cobalt Phthalocyanine. *ACS Energy Lett.* **2018**, *3* (6), 1381–1386. https://doi.org/10.1021/acsenergylett.8b00519.

(54) Torbensen, K.; Han, C.; Boudy, B.; von Wolff, N.; Bertail, C.; Braun, W.; Robert, M. Iron Porphyrin Allows Fast and Selective Electrocatalytic Conversion of CO2 to CO in a Flow Cell. *Chem. - A Eur. J.* **2020**, *26* (14), 3034–3038. https://doi.org/10.1002/chem.202000160.

(55) Walsh, J. J.; Neri, G.; Smith, C. L.; Cowan, A. J. Water-Soluble Manganese Complex for Selective Electrocatalytic CO2 Reduction to CO. *Organometallics* **2019**, *38* (6), 1224–1229. https://doi.org/10.1021/acs.organomet.8b00336.

(56) Costentin, C.; Drouet, S.; Robert, M.; Savéant, J.-M. Turnover Numbers, Turnover Frequencies, and Overpotential in Molecular Catalysis of Electrochemical Reactions. Cyclic Voltammetry and Preparative-Scale Electrolysis. *J. Am. Chem. Soc.* **2012**, *134* (27), 11235–11242. https://doi.org/10.1021/ja303560c.

(57) Rountree, E. S.; McCarthy, B. D.; Eisenhart, T. T.; Dempsey, J. L. Evaluation of Homogeneous Electrocatalysts by Cyclic Voltammetry. *Inorg. Chem.* **2014**, *53* (19), 9983–10002. https://doi.org/10.1021/ic500658x.

(58) Casas, C.; Lacey, C. J.; Meunier, B. Preparation of Hybrid "DNA Cleaver-Oligonucleotide" Molecules Based on a Metallotris (Methylpyridiniumyl)Porphyrin Motif. *Bioconjug. Chem.* **1993**, *4* (5), 366–371. https://doi.org/10.1021/bc00023a011.

(59) Boutorine, A. S.; Brault, D.; Takasugi, M.; Delgado, O.; Hélène, C. Chlorin-Oligonucleotide Conjugates: Synthesis, Properties, and Red Light-Induced Photochemical Sequence-Specific DNA Cleavage in Duplexes and Triplexes. *J. Am. Chem. Soc.* **1996**, *118* (40), 9469–9476. https://doi.org/10.1021/ja960062i.

(60) Stulz, E. Nanoarchitectonics with Porphyrin Functionalized DNA. *Acc. Chem. Res.* **2017**, *50* (4), 823–831. https://doi.org/10.1021/acs.accounts.6b00583.

(61) Llamas, E. M.; Tome, J. P. C.; Rodrigues, J. M. M.; Torres, T.; Madder, A. Porphyrin-Based Photosensitizers and Their DNA Conjugates for Singlet Oxygen Induced Nucleic Acid Interstrand Crosslinking. *Org. Biomol. Chem.* **2017**, *15* (25), 5402–5409. https://doi.org/10.1039/c7ob01269a.

(62) Li, Y.; Gabriele, E.; Samain, F.; Favalli, N.; Sladojevich, F.; Scheuermann, J.; Neri, D. Optimized Reaction Conditions for Amide Bond Formation in DNA-Encoded Combinatorial Libraries. *ACS Comb. Sci.* **2016**, *18* (8), 438–443. https://doi.org/10.1021/acscombsci.6b00058.

(63) Costentin, C.; Robert, M.; Savéant, J. M.; Tatin, A. Efficient and Selective Molecular Catalyst for the CO2-to-CO Electrochemical Conversion in Water. *Proc. Natl. Acad. Sci. U. S. A.* **2015**, *112* (22), 6882–6886. https://doi.org/10.1073/pnas.1507063112.

(64) Karbelkar, A.; Ahlmark, R.; Fan, G.; Yang, V.; Furst, A. 2022. Oxidative Coupling for Facile, Stable Carbon Modification with DNA and Proteins. *ChemRxiv* **2022**, https://doi.org/10.26434/chemrxiv-2022-bt457.

(65) Obermeyer, A. C.; Jarman, J. B.; Netirojjanakul, C.; El Muslemany, K.; Francis, M. B. Mild Bioconjugation through the Oxidative Coupling of Ortho-Aminophenols and Anilines with Ferricyanide. *Angew. Chemie - Int. Ed.* **2014**, *53* (4), 1057–1061. https://doi.org/10.1002/anie.201307386.

(66) Yu, H. Z.; Luo, C. Y.; Sankar, C. G.; Sen, D. Voltammetric Procedure for Examining DNA-Modified Surfaces: Quantitation, Cationic Binding Activity, and Electron-Transfer Kinetics. *Anal. Chem.* **2003**, *75* (15), 3902–3907. https://doi.org/10.1021/ac034318w.

(67) Furst, A.; Hill, M. G.; Barton, J. K. Electrocatalysis in DNA Sensors. *Polyhedron* **2014**, *84*, 150–159. https://doi.org/10.1016/j.poly.2014.07.005.

(68) Chabolla, S. A.; MacHan, C. W.; Yin, J.; Dellamary, E. A.; Sahu, S.; Gianneschi, N. C.; Gilson, M. K.; Tezcan, F. A.; Kubiak, C. P. Bio-Inspired CO2 Reduction by a Rhenium Tricarbonyl Bipyridine-Based Catalyst Appended to Amino Acids and Peptidic Platforms: Incorporating Proton Relays and Hydrogen-Bonding Functional Groups. *Faraday Discuss.* **2017**, *198* (c), 279–300. https://doi.org/10.1039/c7fd00003k.

(69) Walsh, A. P.; Laureanti, J. A.; Katipamula, S.; Chambers, G. M.; Priyadarshani, N.; Lense, S.; Bays, J. T.; Linehan, J. C.; Shaw, W. J. Evaluating the Impacts of Amino Acids in the Second and Outer Coordination Spheres of Rh-Bis(Diphosphine) Complexes for CO2 Hydrogenation. *Faraday Discuss.* **2019**, *215*, 123–140. https://doi.org/10.1039/c8fd00164b.

TOC Graphic

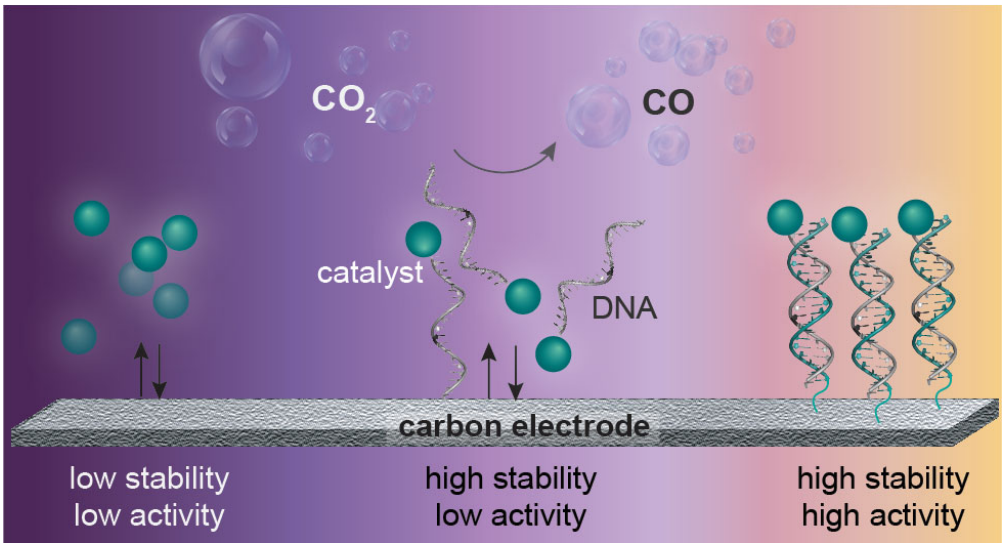

DNA hybridization to immobilize CO_2 reduction catalysts on electrodes improved catalyst stability and efficiency.